Modeling and Minimization of Transceiver Power Consumption in Wireless Networks

Amine Mezghani and Josef A. Nossek
Institute for Circuit Theory and Signal Processing, Technische Universität München, 80290 Munich, Germany
E-Mail: {Mezghani, Nossek}@nws.ei.tum.de

***Abstract*— The minimization of the overall power consumption of wireless networks while satisfying a certain throughput and error rate constraint is investigated. The total power dissipation includes the radiated power as well as the circuit power consumption. In the context of battery operated short range communication, where low power, low cost and small size are key requirements (e.g. standard IEEE 802.15.4), this circuit aware system optimization is crucial given the growing importance of "*Green Communication*". In fact, the power dissipation of certain analog and digital components along the signal path reaches values in the order of or is even higher than the transmit power in such applications. Using an appropriate information-theoretic framework and a simplified wireless network model, we derive the optimal frequency reuse distance, the optimal bit-resolution of the analog-to-digital converter (ADC), the optimal choice of the noise figure for the low noise amplifier (LNA), the optimal operating input back-off (IBO) of the power amplifier (PA), as well as the optimum decoding (DEC) strategy as a function of the path-loss (i.e. the communication distance), that guarantee a certain area spectral efficiency ρ under a certain error probability P_e. This work is an extension to the work [1], [2], [3], where a noisy *single user* channel was assumed.**

I. Introduction

One of the fundamental results of the Shannon's theory is that the minimum transmit signal energy per information bit in an AWGN channel is obtained by taking the bandwidth to infinity and reads as $[E_b/N_0]_{\min} = \ln 2/G_c$, where G_c is the radio path-gain (even though $G_c \leq 1$) and N_0 is the one-sided noise spectral level (in Joule). The classical measure for power efficiency in communications takes only the radiated energy per bit $E_b = P_T/R$ into account. Besides, it is assumed that the receiver has access to the channel data with infinite precision. This classical information theoretic approach is motivated by long range communication and thus neglects the conversion and processing power. However, when communicating over smaller distances using energy-constrained devices (e.g. sensor networks or wireless medical implants), the transmit power can be comparable to the analog/digital processing power. Thus, the power consumption of certain analog and digital components can have a strong impact on the total power consumption. In this paper we aim to jointly minimize the total power consumption of certain transceiver components, in addition to the radiated power, which is motivated by the fact that the transceiver chip transmits and receives almost at the same data rate. To this end, we consider a simplified model of an interference-limited wireless network specified by a certain area spectral efficiency and error rate constraint. The problem of jointly minimizing the transmission and the electronic processing power has been considered in [4], [5] among others. A common assumption is that the power consumption of the circuit components is a constant quantity. The best strategy in that case is to employ bursty transmission with an optimized duty cycle. Nevertheless, the power consumptions of the circuit components are generally mutually coupled with other system parameters (bandwidth, modulation scheme, input back-off, noise power, bit resolution, decoding strategy...) which in turn directly affect the achievable throughput. Other related work is [6] where decoding power is taken into account in addition to the transmission power. Our contribution is in using parametric models for relevant system components in order to get well founded system optimization results (in terms of minimal power consumption). Although the approach includes some simplifications and approximations, the obtained results might show essential trends when communication distances become smaller.

II. Framework Description

Fig. 1 shows a block diagram of a wireless transceiver.

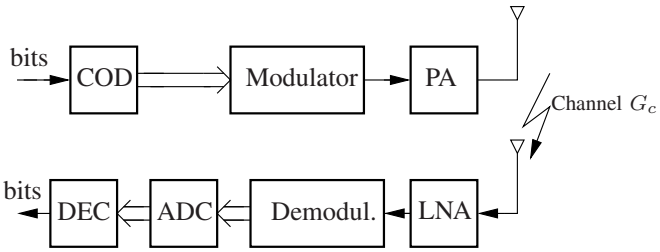

Fig. 1. Components of a SISO transceiver.

The components involved in our power minimization framework are the power amplifier (PA), the low noise amplifier (LNA), the analog-to-digital converter (ADC) and the decoder (DEC). The channel encoding is usually much less complex than decoding and thus we neglect its power dissipation.
In the following, we briefly present the results of our literature search on communication circuits and their modeling [7], [8], [9].

A. Power consumption of the Power Amplifier (PA)

The average power consumption of the power amplifier is denoted by P_{PA} and already includes the average radiated power P_T. They are in fact related by

$$P_T = \eta P_{\mathrm{PA}}, \tag{1}$$

978-1-61284-074-1/11/$26.00 ©2011 IEEE

where $\eta \leq 1$ is the average drain power efficiency of the amplifier. The instantaneous power efficiency usually depends on the ratio of the instantaneous amplitude of the RF sinusoid a_x to the maximum output voltage A. Let consider the simplified push-pull amplifier in Fig. 2, having unit voltage amplification without loss of generality, and let describe it by the following simple model

$$x = a_x \sin(\omega t + \varphi_x) \tag{2}$$

$$u_t = \text{sign}(\sin(\omega t + \varphi_x)) \cdot \min(|a_x \sin(\omega t + \varphi_x)|, A) \tag{3}$$

$$i_L \approx I_L \sin(\omega t + \varphi_x) \tag{4}$$

$$i_d = |i_L|, \tag{5}$$

where ω is the carrier frequency. Furthermore, we take soft-limiter type of nonlinearity as an approximation for the input-output characteristic

$$y = R_L \cdot i_L \approx \min(a_x, A) \sin(\omega t + \varphi_x). \tag{6}$$

For a complex Gaussian input alphabet with variance σ_x^2 the amplitude a_x is Rayleigh distributed

$$f_{a_x}(a_x) = \frac{2a_x}{\sigma_x^2} \exp(-\frac{a_x^2}{\sigma_x^2}), \tag{7}$$

and we obtain the average PA power consumption from (6) and (5) ($R_L = 1$ without loss of generality)

$$\begin{aligned} P_{\text{PA}} &= \text{E}[A \cdot i_d] \\ &= \int_0^A A a_x f_{a_x}(a_x) da_x + \int_A^\infty A^2 f_{a_x}(a_x) da_x \\ &= \frac{\sqrt{\pi} z}{2} \text{erf}(z) \sigma_x^2, \end{aligned} \tag{8}$$

where $z = \frac{A}{\sigma_x}$ represents the Input back-off (IBO) of the power amplifier.

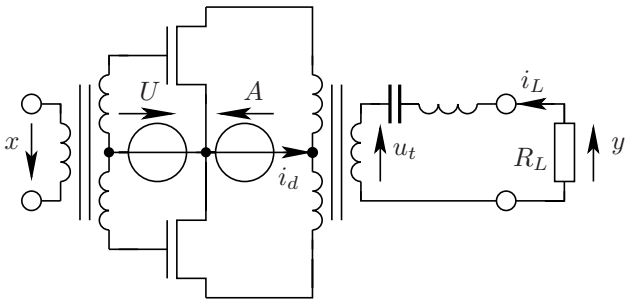

Fig. 2. Simplified push-pull transformer amplifier.

Obviously, there is a trade-off between power efficiency and the signal distortion due to clipping. To quantify the distortion effects we decompose the output of the amplifier y given in (6) into a desired signal component and an uncorrelated distortion n_{PA} using the Bussgang theorem

$$y = \alpha \cdot x + n_{\text{PA}}. \tag{9}$$

For a given IBO z, α and the variance of n_{PA} take under the distribution (7) the values

$$\alpha = 1 - \text{e}^{-z^2} + \frac{\sqrt{\pi} z}{2} \text{erfc}(z), \tag{10}$$

and

$$\sigma_{n_{\text{PA}}}^2 = (1 - \text{e}^{-z^2} - \alpha^2) \sigma_x^2. \tag{11}$$

Finally, the radiated power turns to be

$$P_T = \alpha^2 \sigma_x^2 + \sigma_{n_{\text{PA}}}^2 = (1 - \text{e}^{-z^2}) \sigma_x^2, \tag{12}$$

and we have the PA efficiency

$$\eta = \frac{P_T}{P_{\text{PA}}} = \frac{2(1 - \text{e}^{-z^2})}{\sqrt{\pi} z \text{erf}(z)}. \tag{13}$$

B. Power consumption of the low noise amplifier (LNA)

Although, there are many performance factors in LNAs, we concentrate on four important parameters such as power gain, bandwidth, noise figure and power dissipation. These are included in a figure-of-merit expression FOM_{LNA} [10]

$$\text{FOM}_{\text{LNA}} = \frac{G_{\text{LNA}} \cdot B \cdot N_0}{(N_F - 1) \cdot P_{\text{LNA}}}, \tag{14}$$

where G_{LNA} is the power gain, N_F is the noise figure, P_{LNA} is the power consumption and B is the operating bandwidth. Note that we multiplied the figure-of-merit definition in [10] by N_0, just to make it dimensionless. A noise figure of value N_F means that the LNA enhances the thermal noise level N_0 by the factor N_F. It turns out that for "good" designed LNAs the FOM_{LNA} can be considered as an invariant quantity that only depends on the process technology and certain transistor parameters, and thus can not be influenced by our system optimization. Recent LNA designs found in the literature exhibit an FOM_{LNA} in the range of 10^{-7} to 10^{-9}. The gain G_{LNA} is not subject of the optimization and is set to 10, so that the effect of noise from subsequent stages can be neglected.

C. Power consumption of the A/D Converter (ADC)

The ADC complexity grows with the resolution b and the bandwidth B and it heavily affects the complexity of the following digital signal processing, e.g. the required memory size. In fact, it has been observed that new ADC architectures like pipelined ADCs are thermal noise limited and thus their minimum possible power is proportional to $N_0 \cdot 2^{2b} \cdot f_s$, where f_s is the sampling frequency [8] (see Fig. 3). In other words, under Nyquist rate sampling, the power needed for converting a complex signal with bandwidth B can be modeled as (see [8] for further motivation):

$$P_{\text{ADC}} = 2 \cdot c_{\text{ADC}} \cdot N_0 \cdot 2^{2b} \cdot B, \tag{15}$$

with some proportionality constant c_{ADC} depending on the ADC architecture. Although (15) is still not representative for the broad amount of actual ADC designs (especially at low resolution), it can be seen as the fundamental limit on conversion power due to thermal noise. Eq. (15) results in a trade-off between power consumption and performance loss due to quantization. It is therefore of interest to design the system parameters like bandwidth and ADC resolution in order to minimize the total power consumption including the conversion power.

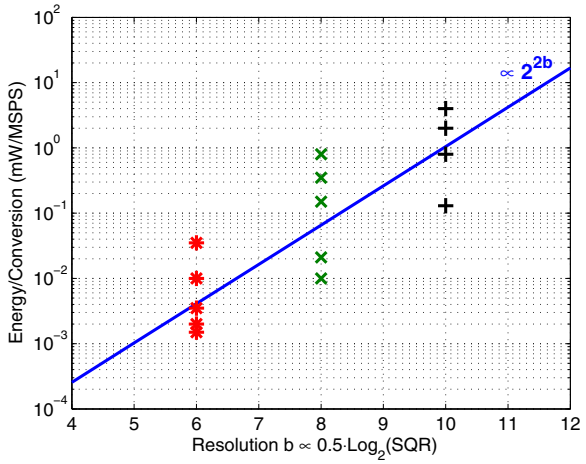

Fig. 3. Power consumption of recent ADCs found in the literature.

D. Power consumption of the channel decoder (DEC)

Let us consider for instance low density parity check (LDPC) codes which are emerging in many new applications and standards. A regular binary (N, λ, γ) LDPC block code [11] is described by an $N \times K$ parity check matrix. N is the number of variable nodes (i.e. the block length), K is the number of check nodes, whereas λ is the number of edges connected to each variable nodes (i.e. the number of ones in each column) and γ is the number of edges connected to each check nodes (i.e. the number of ones in each row). Hence, the number of useful information bits is $N - K$ and the LDPC code rate is given by

$$r_{\mathrm{COD}} = 1 - \frac{K}{N} = 1 - \frac{\lambda}{\gamma}. \tag{16}$$

Each iteration of the decoding algorithm, well-known as belief propagation, consists in, first sending messages from each variable node to each adjacent check node, and then vice versa. The messages contain the extrinsic information of each information bits in form of density functions computed based on the previously received messages (see Fig. 4). Let assume the energy consumed by computing and exchanging messages over one edge at each iteration, E_{edge}, to be a constant parameter, then the total energy consumption of decoding one block with ℓ iterations is roughly

$$E_{\mathrm{DEC}} = E_{\mathrm{edge}} \cdot \lambda \cdot N \cdot \ell. \tag{17}$$

Typical values for E_{edge} extracted from the literature are in the range $10^7 \cdot N_0$ to $10^8 \cdot N_0$ (when taking $N_0 = k_B \cdot T$). Please refer to [9] and the references therein for more precise energy modeling of LDPC decoders. Now, under a certain target information rate R (in bits/sec) the power consumption of the decoder can be obtained as

$$P_{\mathrm{DEC}} = \frac{E_{\mathrm{DEC}}}{N-K} R = E_{\mathrm{edge}} \cdot \lambda \cdot \frac{1}{r_{\mathrm{COD}}} \cdot \ell \cdot R. \tag{18}$$

Since the $r_{\mathrm{COD}} < 1$ and the overall code rate (or bandwidth efficiency in bits/channel use) is obtained from the combination of the modulation order $L \geq 2$ (any modulation alphabet includes at least 2 symbols) and the channel code rate as

$$r = \frac{R}{B} = r_{\mathrm{COD}} \log_2 L, \tag{19}$$

we get $r_{\mathrm{COD}} < \min\{1, r\}$, and we can deduce a lower bound on the decoding power consumption as function of the target rate and the bandwidth

$$P_{\mathrm{DEC}} = E_{\mathrm{edge}} \cdot \lambda \cdot \max\{R, B\} \cdot \ell. \tag{20}$$

In many applications, besides of the target rate, a certain maximum error probability P_e is specified. Therefore we need to evaluate the performance of the LDPC code in terms of achievable error rate. In [12], it has been shown that the error probability for regular LDPC codes under iterative decoding can decreases double-exponentially with the iteration index ℓ as long as $\ell < \frac{\log(N)}{\log(\lambda-1)\log(\gamma-1)}$, that is

$$P_e \approx 2^{-E_r(\lambda-1)^\ell}, \tag{21}$$

for a certain constant error exponent E_r, which is difficult to be determined in general. Motivated by the simple characterization of the error exponent for random codes [13], we approximate E_r by the difference between the theoretic achievable rate r_0 (or channel capacity), which will be discussed next, and the actual overall code rate $r = R/B$ (both in bits/channel use), i.e., $E_r = r_0 - r$. All in all, the decoding power as function of the system specifications is

$$P_{\mathrm{DEC}} = \lambda E_{\mathrm{edge}} \max(R, B) \log_{\lambda-1}\left(\frac{-\log_2 P_e}{r_0 - R/B}\right). \tag{22}$$

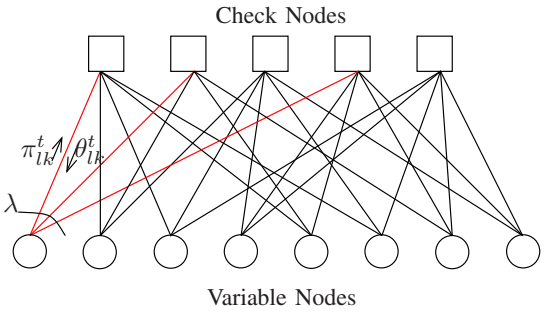

Fig. 4. Tanner graph representing of the LDPC ocde.

E. Achievable Rate

Taking into account the distortion noise caused by the power amplifier and the noise figure of the LNA, we obtain the effective SNR as

$$\mathrm{SNR} = \frac{G_c \cdot \alpha^2 \cdot \sigma_x^2}{G_c \cdot \sigma^2_{n_{\mathrm{PA}}} + N_F \cdot N_0 \cdot B}. \tag{23}$$

Let us now consider a simplified wireless network as shown in Fig. 5, which is a collection of several unfaded point-to-point links (no multi-hop relaying). To limit interference, the total available bandwidth (denoted by B) is divided into different sub-bands allocated to different neighboring users. For the sake of simplicity and tractability, a coordinated frequency

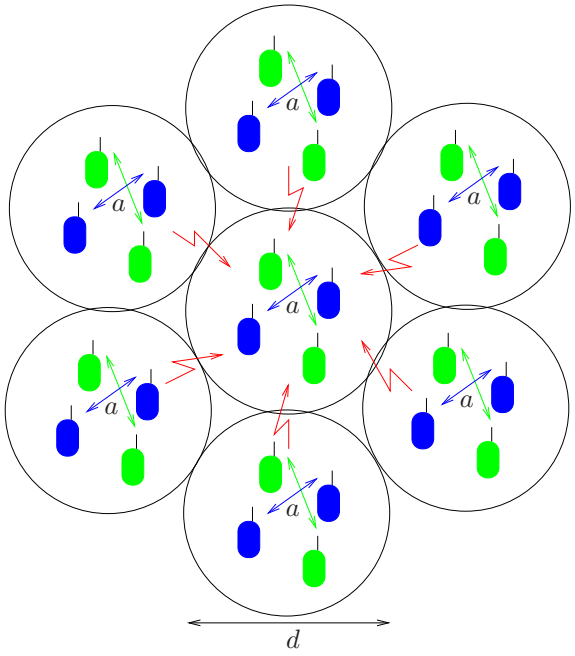

Fig. 5. A wireless network containing a set of point-to-point links. a is the communication distance, d is the frequency reuse distance, that is the distance between the nearest communication pairs using the same sub-band.

reuse is assumed, where the frequency reuse distance is denoted by d, which will be also optimized. This assumption is strictly speaking not realistic in a real uncoordinated (non-cellular) network, but can be approached by intelligent sub-band sensing and selection techniques. Nevertheless, we will see later that some results presented in [14] for a more realistic setting and based on stochastic geometry can be recovered for the ideal case, i.e. where only transmission power is taken into account, which might justify the usefulness of this simple model. For the optimization, the following network properties are assumed:

- users locations are uniform distributed,
- interference links using the same band is treated as noise,
- a fixed transmitter-receiver distance a,
- a total available bandwidth B,
- a target area bandwidth efficiency ρ [bit/s/Hz/m^2],
- a target error probability P_e,
- a pathloss model given by $G_c = \min\{\frac{G_{1\mathrm{m}}}{(a/1\mathrm{m})^\kappa}, 1\}$, with path-loss exponent κ (no fading).

Given these assumptions, we just have to adapt the SNR formula in (23) to include the interference term and get the signal-to-interference-plus-noise-ratio (SINR):

$$\mathrm{SINR} = \frac{G_c \cdot \alpha^2 \cdot \sigma_x^2}{G_c \cdot \sigma_{n_{\mathrm{PA}}}^2 + N_F \cdot N_0 \cdot B + I(P_T, d)}, \tag{24}$$

where $I(P_T, d)$ is the interference term which is function of the total radiated power (cf. (1)) in one "virtual" cell of size d, i.e. the frequency reuse distance. Assuming uniformly distributed power over the area, we approximate the total interference as

$$I(P_T, d) = \int_{\frac{d}{2}}^{\infty} \frac{P_T}{\pi d^2/4} \frac{G_{1\mathrm{m}}}{(x/1\mathrm{m})^\kappa} 2\pi x dx = \frac{2P_T}{\kappa - 2} \frac{G_{1\mathrm{m}}}{(d/2\mathrm{m})^\kappa}. \tag{25}$$

On the other hand, in [15], a lower bound on the achievable channel capacity under output quantization by means of an MMSE approach has been derived, as follows

$$r_0 \geq \log_2 \left(\frac{1 + \mathrm{SINR}}{1 + \mathrm{SINR}/\mathrm{SQR}} \right), \tag{26}$$

where SQR is the signal-to-distortion ratio related to the ADC resolution b. This bound is tight at low SINR and its derivation does not assume uncorrelated additive quantization noise. In order to maximize SQR, an AGC-circuit is placed before the ADCs, which scales the noisy inphase and quadrature signals by a factor such that the ADCs are driven with an optimal input power. In this case, $\mathrm{SQR} \propto 2^{2b}$ and we can approximate the channel capacity under finite resolution b as

$$r_0 \approx \log_2 \left(\frac{1 + \mathrm{SINR}}{1 + \mathrm{SINR} \cdot 2^{-2b}} \right), \tag{27}$$

which is consistent with the fact, that the achievable rate per channel use with infinite SINR is $2b$. The ADC resolution is commonly chosen such that the ADC distortion noise is about 10dB below the overall noise level. However, such an approach is inappropriate for designing low power systems.

III. Total Power Minimization

Using the above energy consumption models, we aim to jointly minimize the transmission and the analog processing power consumption with respect to the different system parameters (resolution, frequency reuse, noise figure, input back-off). The considered setting includes a bandwidth limitation denoted by B. We aim also to determine the fractions of power that should be optimally allocated to each of the components (PA, LNA, ADC, DEC). Let us consider the total power spent in the transmission,

$$P_{\mathrm{total}} = P_{\mathrm{PA}} + P_{\mathrm{ADC}} + P_{\mathrm{LNA}} + P_{\mathrm{DEC}}. \tag{28}$$

Our goal is in fact to minimize the energy per communicated bit $E_b = P_{\mathrm{total}}/R$ for a given target area spectral efficiency ρ [bit/s/Hz/m^2] and a maximal error probability P_e,

$$\min_{d,b,z,N_F,\ell} \frac{P_{\mathrm{total}}}{R} \text{ st. } \frac{R}{B\pi d^2/4} \geq \rho \text{ and } \Pr(\mathrm{error}) \leq P_e. \tag{29}$$

Hereby R and P_{total} are the total transmission rate and the total power consumption in one "virtual" cell of size d, respectively. The optimization should be performed with respect to the frequency reuse distance d, the IBO z of the PA, the noise figure N_F of the LNA, the resolution b of the ADC and the number of decoding iterations ℓ. Evidently, the parameter λ of the LDPC code can be also optimized but it is considered to be fixed here. Using numerical optimization methods, the global optimizer of this function is easily found, since only a relatively small number of parameters are involved.

IV. Numerical Results

As an example, let us take a path-loss exponent $\tau = 3.5$, $c_{\mathrm{ADC}} = 10^5$, which is a typical value of recent comparator-based ADCs [8], $\mathrm{FOM}_{\mathrm{LNA}} = 10^{-7}$ [10], while the decoder is specified by $\lambda = 6$, $E_{\mathrm{edge}} = 10^7 \cdot N_0$ and a target error probability $P_e = 10^{-14}$.

First of all, in Fig. 6 the required energy per bit is considered for $G_c = -65$dB and $G_c = -75$dB as function of the the quantity $\rho \cdot a^2$ [in bit/s/Hz], which we refer to as network intensity, i.e. the product of the area spectral efficiency and the squared communication distance. This quantity might be crucial to differentiate two operating regions. In the first one where $\rho \cdot a^2 \leq 0.2$, the energy per bit E_b does not depend much on the rate, which is typical for a noise-limited network (low to medium interference). In the second one, the network intensity saturates and approaches the maximal value of 0.289 and E_b increased drastically, indicating an interference-limited scenario (interference much stronger than noise). For comparison, we also plotted the corresponding (G_c-independent) curves for the ideal case, where only the radiated power is minimized, and for uncoded QPSK transmission, which performs better at low network intensity and short range but is obviously useless in the interference-limited regime. This shows the importance of channel coding in wireless networks even in short range applications. Note that similar observations have been done in [6].

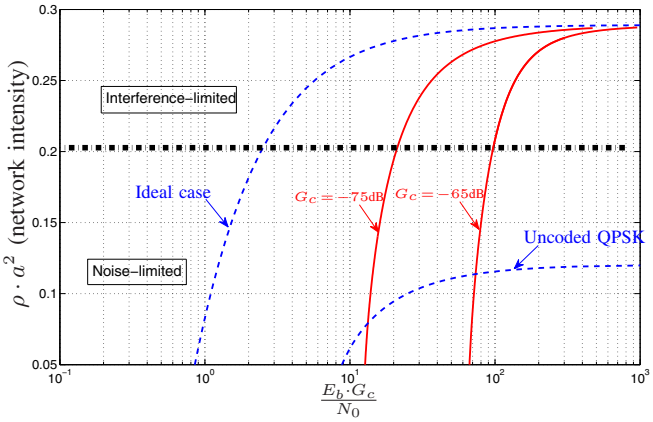

Fig. 6. Total energy per bit E_b vs. network intensity, $\tau = 3.5$.

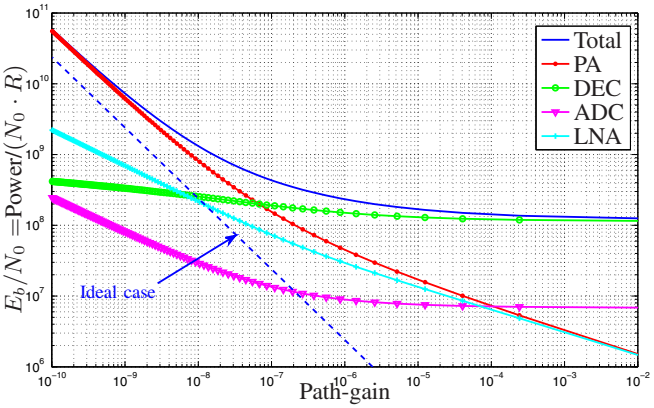

Fig. 7. Normalized energies per bit vs. the path-gain, $\rho \cdot a^2 = 0.2$, $\tau = 3.5$.

Noise-limited scenario: let us now vary the path gain G_c, or in other words the communication distance a, while maintaining $\rho \cdot a^2 = 0.2$ fixed, which corresponds rather to a noise-limited (medium interference) case. The normalized combined energy per bit required to communicate across the wireless network is depicted in Fig. 7. The term $\frac{P_{\mathrm{total}}}{N_0 R}$ corresponds to the minimal energy per bit normalized by N_0. The fractions of energy per bit needed by each component are also illustrated. Remarkably, even at a very small path-loss, the required total energy per bit is quite large due to the decoding power consumption. Observe that, only for very small G_c (long range communication), the transmission power is dominant, in accordance to the classical approach, while for high G_c (short range communication), the decoding power becomes dominant. As already mentioned, for large G_c, the ADC power becomes significant compared to the transmit power but remains smaller than the decoding power. On the other hand, the fraction of power that should be dedicated to the LNA remains insignificant even for high path-gains. All in all, at very short communication distances, the decoding power is dominant. The behavior of the bandwidth efficiency (net bit rate R divided by the bandwidth B) versus the path-gain is shown in Fig. 8. Interestingly, the optimal operating bandwidth efficiency in the medium and high path-gain range takes values between 1 and 2 bits per channel use (bpcu), which are quite common in the practice. Additionally, the channel capacity r_0 from (26) is also depicted, showing that operating codes away from capacity is optimal. Fig. 9 shows the optimal operating IBO of the power amplifier. At short distances, it is advantageous to operate the PA at high IBO values, i.e., at low drain efficiency, in order to reduce the distortion effects, due to the negligible PA power dissipation. On the other hand, Fig. 10 shows, that the optimal resolution for short range communication is indeed quite low and is about 3 bit. This suggests, that low resolution ADCs may be a good choice for low power short range and noise-limited communications. The optimal choice of the noise figure for the LNA is shown in Fig. 11. Clearly, there is no advantage from putting a lot of effort to reduce the noise figure at a high channel gain, i.e., at short communication distances, since this would require much higher LNA power relatively to the transmission power. Fig. 12 illustrates the optimal number of decoding iterations. As expected, this number should be decreased with increasing path-gain in order to reduce the power dissipation mainly due to the decoder. Finally, Fig. 13 shows the optimal reuse distance d normalized by the communication distance which interestingly increases with path-gain, in order to reduce interference and thus facilitate the receive processing.

Interference-limited scenario: we now choose $\rho \cdot a^2 =$

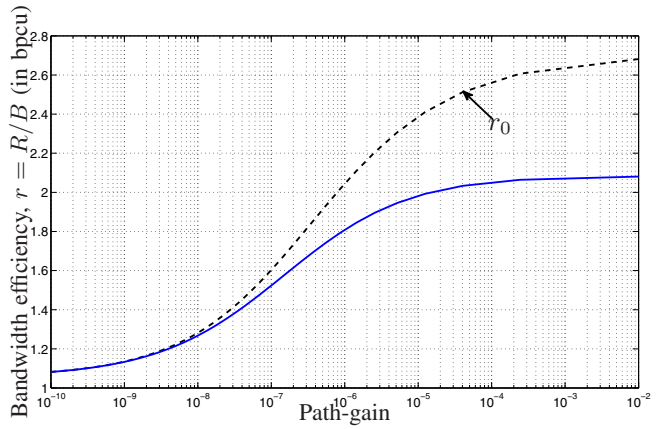

Fig. 8. Optimal bandwidth efficiency vs. the path-gain, $\rho a^2 = 0.2$, $\tau = 3.5$.

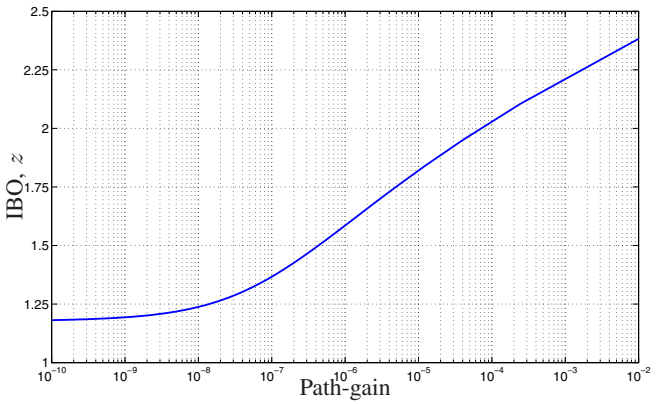

Fig. 9. Optimal operating IBO vs. the path-gain, $\rho \cdot a^2 = 0.2$, $\tau = 3.5$.

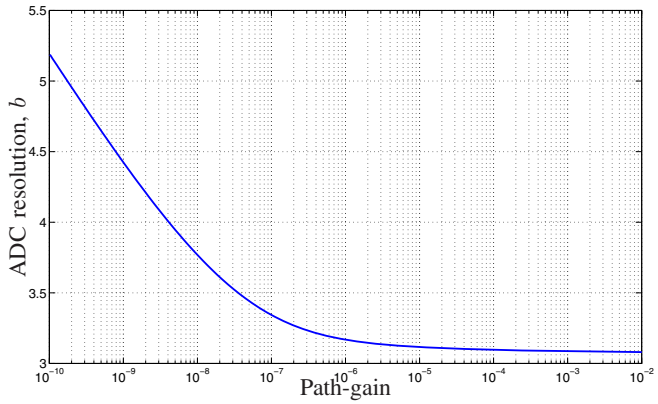

Fig. 10. Optimal ADC resolution vs. the path-gain, $\rho \cdot a^2 = 0.2$, $\tau = 3.5$.

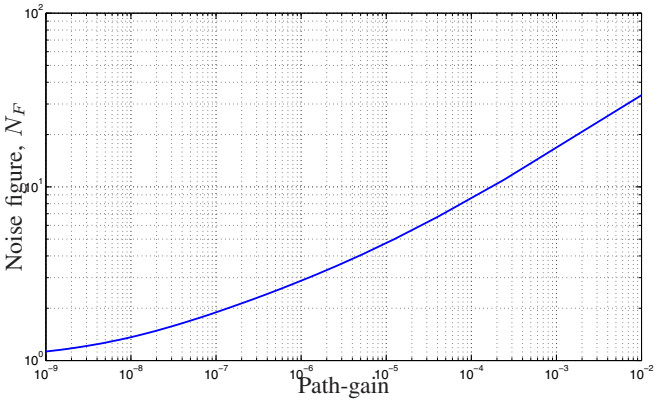

Fig. 11. Optimal noise figure vs. the path-gain, $\rho \cdot a^2 = 0.2$, $\tau = 3.5$.

0.289, which is here a strongly interference-limited case. The normalized combined energy per bit is plotted again in Fig. 14. Obviously, significantly higher E_b is needed compared to the first scenario regardless of the path-gain. The optimizing values for the IBO, ADC resolution, noise figure and number of decoding iterations are depicted in Fig. 15-18, respectively. As we can see, the components requirements become more strict compared to the noise-limited case.

V. Power efficiency in strongly interference-limited wireless networks

When comparing Fig. 14 to Fig. 7 we observe that, when converging to strongly interference-limited regime (maximal network intensity $\rho \cdot a^2$), the power consumptions of PA and ADC dominate progressively the total power consumption regardless of the path-gain, due to the high resolution needed. This motivates us to consider a simplified power efficiency problem that takes only the ADC and the PA into account. For simplicity an ideal PA is assumed with $P_T = P_{\mathrm{PA}}$ and without non-linearity effects. As mentioned earlier, the achievable spectral efficiency in an interference network when taking finite resolution into account is

$$r_0 \approx \log_2\left(\frac{1+\mathrm{SINR}}{1+\mathrm{SINR}\cdot 2^{-2b}}\right) = \log_2\left(\frac{\frac{1}{\mathrm{SNR}}+\frac{1}{\mathrm{SIR}}+1}{\frac{1}{\mathrm{SNR}}+\frac{1}{\mathrm{SIR}}+2^{-2b}}\right), \tag{30}$$

where the SNR is now given by

$$\mathrm{SNR} = \frac{G_c P_T}{B N_0}, \tag{31}$$

and using (25)

$$\mathrm{SIR} = \frac{G_c P_T}{I(P_T, d)} = \frac{\kappa - 2}{2}\left(\frac{d}{2a}\right)^{\kappa}. \tag{32}$$

Now, we assume a total power budget $P_{\mathrm{total}} = P_T + P_{\mathrm{ADC}}$ and we introduce the ratio $\mu = \frac{P_{\mathrm{ADC}}}{P_T}$, which we aim to optimize. Then, (30) can be rewritten as

$$r_0 \approx \log_2\left(\frac{\xi\frac{1+\mu}{2c_{\mathrm{ADC}}G_c}+\frac{1}{\mathrm{SIR}}+1}{\xi\frac{1+\mu}{2c_{\mathrm{ADC}}G_c}+\frac{1}{\mathrm{SIR}}+\xi\frac{1+\mu}{\mu}}\right), \tag{33}$$

where $\xi = 2c_{\mathrm{ADC}} B N_0 / P_{\mathrm{total}}$. Next, taking the derivative of r_0 with respect of μ, we obtain the following optimality

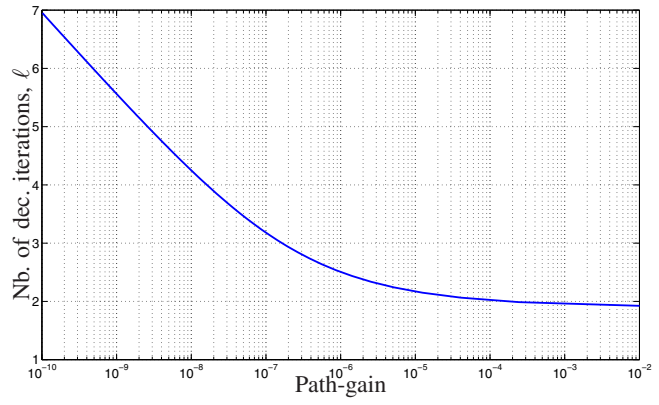

Fig. 12. Optimal number of dec. iterations vs. the path-gain, $\rho \cdot a^2 = 0.2$, $\tau = 3.5$.

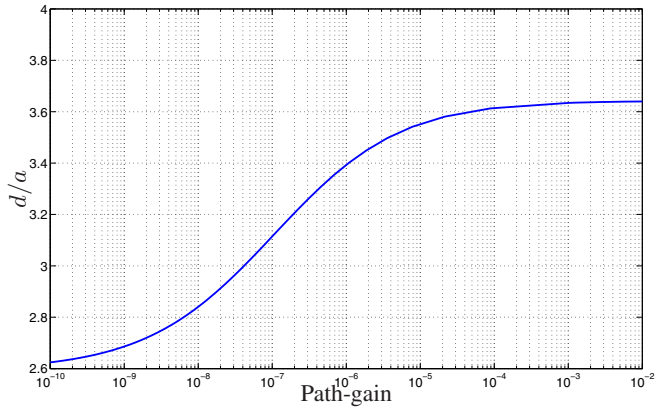

Fig. 13. Optimal ratio d to a vs. the path-gain, $\rho \cdot a^2 = 0.2$, $\tau = 3.5$.

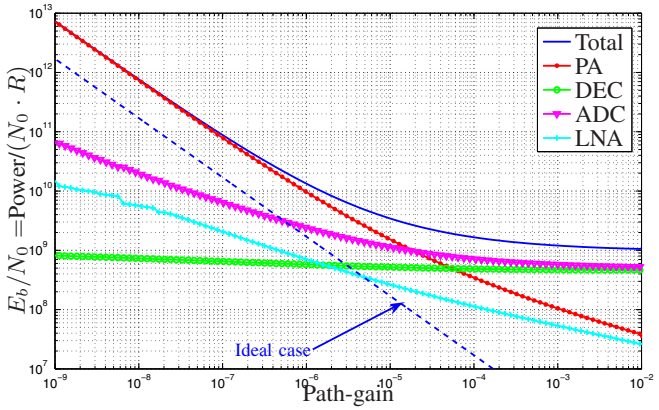

Fig. 14. Normalized energies per bit vs. the path-gain, $\rho a^2 = 0.289$, $\tau = 3.5$.

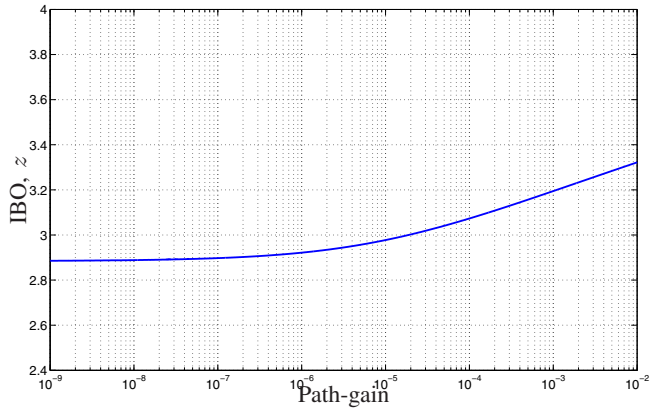

Fig. 15. Optimal operating IBO vs. the path-gain, $\rho a^2 = 0.289$, $\tau = 3.5$.

condition

$$\frac{\xi}{2c_{\mathrm{ADC}}G_c}\left(\xi\frac{1+\mu}{2c_{\mathrm{ADC}}G_c}+\frac{1}{\mathrm{SIR}}+\xi\frac{1+\mu}{\mu}\right)- \tag{34}$$

$$\left(\frac{\xi}{2c_{\mathrm{ADC}}G_c}-\frac{\xi}{\mu^2}\right)\left(\xi\frac{1+\mu}{2c_{\mathrm{ADC}}G_c}+\frac{1}{\mathrm{SIR}}+1\right)\stackrel{!}{=}0. \tag{35}$$

After some algebraic manipulations to solve last equation, we get the optimal conversion-to-transmit power ratio μ

$$\frac{P_{\mathrm{ADC}}}{P_T}=\frac{\xi}{1-\xi}+\sqrt{\frac{2c_{\mathrm{ADC}}G_c}{1-\xi}(1+\frac{1}{\mathrm{SIR}})+\frac{\xi}{(1-\xi)^2}}, \tag{36}$$

where again $\xi = 2c_{\mathrm{ADC}}BN_0/P_{\mathrm{total}}$. In the strongly interference-limited regime (high power, high resolution and finite bandwidth) we get the optimal ratio as

$$\left.\frac{P_{\mathrm{ADC}}}{P_T}\right|_{\xi\to 0}=\sqrt{2c_{\mathrm{ADC}}G_c(1+\frac{1}{\mathrm{SIR}})}. \tag{37}$$

Since $\mathrm{SIR}\propto(d/a)^{\kappa}$ (cf. (32)), then the area spectral efficiency [in bit/s/Hz/m^2] in the strongly interference-limited regime ($\xi\to 0$) is given by

$$\rho\ [\text{in bit/s/Hz/m}^2]\propto\frac{1}{d^2}\log(1+\mathrm{SIR})\propto\mathrm{SIR}^{-\frac{2}{\kappa}}\log(1+\mathrm{SIR}). \tag{38}$$

Maximizing this area spectral efficiency yields the optimal operating SIR as [14]

$$\mathrm{SIR}_{\mathrm{opt}}=\mathrm{e}^{\frac{\kappa}{2}+\mathrm{W}(-\frac{\kappa}{2}\mathrm{e}^{-\frac{\kappa}{2}})}-1, \tag{39}$$

where $W(\cdot)$ denotes the Lambert function verifying the identity $W(y)\mathrm{e}^{W(y)}=y$. Numerical results of this optimal transmission-to-conversion power ratio vs. the path gain G_c is shown in Fig. 19 for different path-loss exponents. We observe that the ADC power dissipation becomes dominant when the path-gain exceed -50dB.

VI. Conclusion

We have presented a circuit-aware design framework for energy efficient communication networks that takes into account the characteristics and the power consumptions of the PA, LNA, ADC, DEC. In the context of short range communication, we showed that, the channel decoder dominates the total power consumption under the state-of-the-art technology in the low to medium interference (i.e. noise-limited) regime, while the ADC power dissipation becomes significant in the strongly interference-limited regime due to the high resolution requirements. On the other hand, in the noise-limited regime and even in the moderate interference-regime, low-resolution

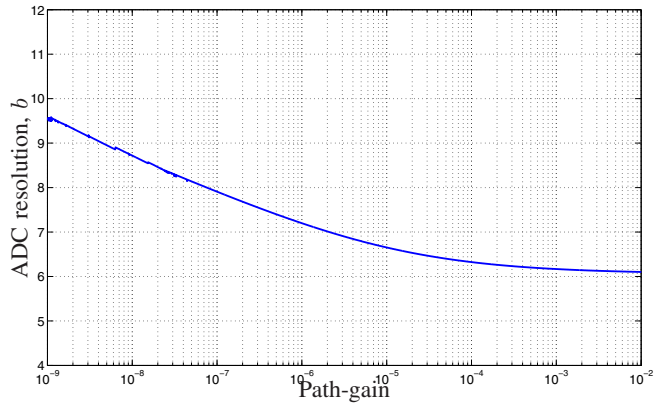

Fig. 16. Optimal ADC resolution vs. the path-gain, $\rho a^2 = 0.289$, $\tau = 3.5$.

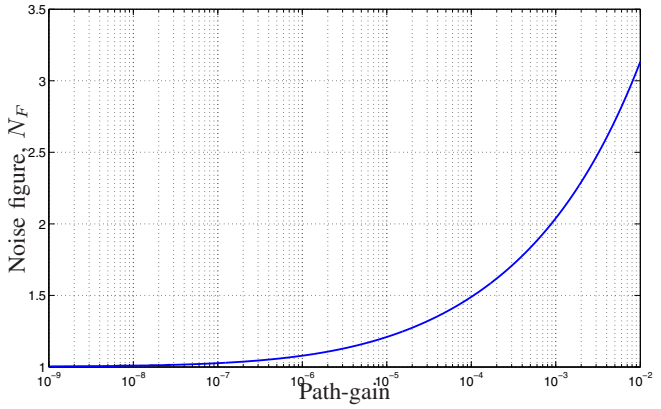

Fig. 17. Optimal noise figure vs. the path-gain, $\rho a^2 = 0.289$, $\tau = 3.5$.

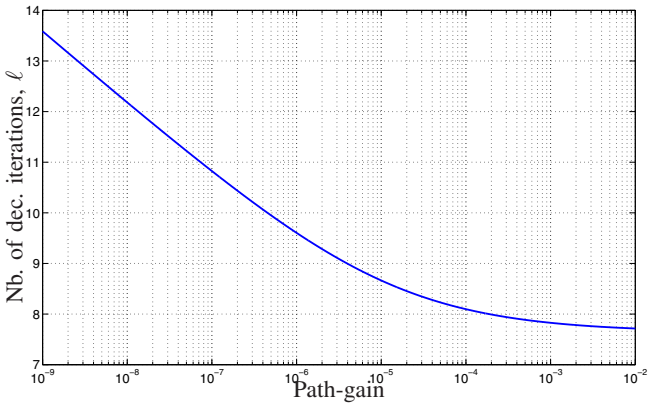

Fig. 18. Optimal number of dec. iterations vs. the path-gain, $\rho a^2 = 0.289$, $\tau = 3.5$.

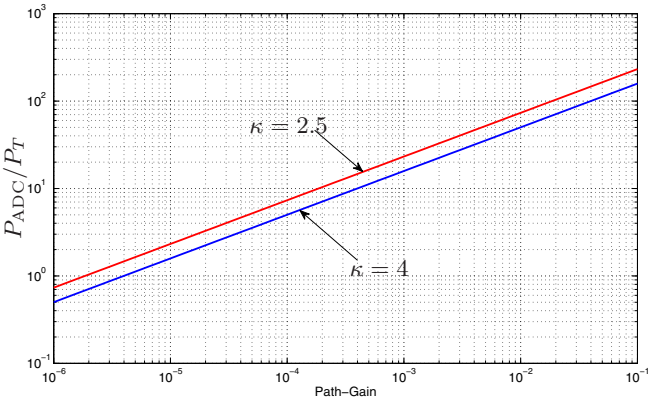

Fig. 19. Optimal ADC to transmit power ratio, $\kappa = 2.5$ and $\kappa = 4$, interference-limited regime.

sampling exhibits a good performance, while reducing the total power consumption. In general, it is also beneficial for short communication distances to design LNAs with poor noise figure in terms of overall power consumption. Additionally, in contrast to single isolated links, the role of channel coding is crucial in wireless network regardless of the range. We believe that these results also hold for more general channel settings, e.g. MIMO channels.

REFERENCES

[1] A. Mezghani and J. A. Nossek, "How to choose the ADC resolution for short range low power communication?," in *Proc. ISCAS*, Paris, France, May 2010.

[2] A. Mezghani, N. Damak, and J. A. Nossek, "Circuit Aware Design of Power Efficient Short Range Communication Systems," in *Proc. ISWCS*, York, UK, September 2010.

[3] A. Mezghani and J. A. Nossek, "Power Efficiency in Communication Systems from a Circuit Perspective," in *accepted for ISCAS*, Rio de Janeiro, Brazil, May 2011.

[4] S. Cui, A. Goldsmith, and A. Bahai, "Energy-constrained modulation optimization," *IEEE Trans. Wireless Commun.*, vol. 4, no. 5, pp. 2349–2360, September 2005.

[5] Florian Trösch, Christoph Steiner, Thomas Zasowski, Thomas Burger, and Armin Wittneben, "Hardware aware optimization of an ultra low power UWB communication system," in *IEEE International Conference on Ultra-Wideband, ICUWB 2007*, Sept. 2007.

[6] P. Grover, K. Ann Woyach, and A. Sahai, "Towards a communication-theoretic understanding of system-level power consumption," *submitted to IEEE Journal on Selected Areas in Communications*, 2010, available at http://arxiv.org/.

[7] Thomas H. Lee, *The Design of CMOS Radio-Frequency Integrated Circuits*, Cambridge University Press, second edition, 2003.

[8] H. S. Lee and C. G. Sodini, "Analog-to-Digital Converters: Digitizing the Analog World," *Proceedings of the IEEE*, vol. 96, no. 2, pp. 323–334, February 2008.

[9] M. Korb and T. G. Noll, "LDPC Decoder Area, Timing, and Energy Models for Early Quantitative Hardware Cost Estimates," in *Proc. ISSoC*, Tampere, Finland, September 2010.

[10] Y.-H. Yu, Y.-J. E. Chen, and D. Heo, "A 0.6-V Low Power UWB CMOS LNA," *IEEE microwave and wireless components letters*, vol. 17, no. 3, pp. 229–231, March 2007.

[11] D. J. C. MacKay, "Good error-correcting codes based on very sparse matrices," *IEEE Trans. Inf. Th.*, vol. 45, no. 2, pp. 399–431, Mar. 1999.

[12] M. Lentmaier, D. Truhachev, K. Zigangirov, and D. Costello, "An analysis of the block error probability performance of iterative decoding," *IEEE Trans. Inf. Th.*, vol. 51, no. 11, pp. 3834–3855, Nov. 2005.

[13] R. G. Gallager, *Information Theory and Reliable Communication*, New York: JohnWiley and Son, 1968.

[14] N. Jindal, J.G. Andrews, and S. Weber, "Optimizing the SINR operating point of spatial networks," in *Proc. Information Theory and its Applications Workshop (ITA)*, San Diego, CA, January 2007.

[15] A. Mezghani, M. S. Khoufi, and J. A. Nossek, "A Modified MMSE Receiver for Quantized MIMO Systems," *In Proc. ITG/IEEE WSA, Vienna, Austria*, February 2007.